Dean Falk*, John C. Redmond, Jr and John Guyer
Department of Anthropology, University at Albany, SUNY, Albany, NY 12222, U.S.A. E-mail: D.Falk@Albany.edu; Redmond@empireone.net; Jguyer@capital.net

Glenn C. Conroy
Departments of Anatomy and Neurobiology/Anthropology, Washington University School of Medicine, St Louis, MO 63110, U.S.A. E-mail: Conroyg@thalamus.wustl.edu

Wolfgang Recheis
Department of Radiology II, University of Innsbruck, Anichstr. 35, A-6020, Innsbruck, Austria. E-mail: Wolfgang.recheis@uibk.ac.at

Gerhard W. Weber and Horst Seidler
Institute of Human Biology, University of Vienna, Althanstrasse 14, A1091, Vienna, Austria. E-mail: Gerhard.weber@univie.ac.at; Horst.seidler@univie.ac.at

Received 6 May 1999
Revision received 2 August 1999 and accepted 5 November 1999

Keywords: *Australopithecus*, endocasts, frontal lobe, paleoneurology, *Paranthropus*, phylogeny, temporal lobe.

Early hominid brain evolution: a new look at old endocasts

Early hominid brain morphology is reassessed from endocasts of *Australopithecus africanus* and three species of *Paranthropus*, and new endocast reconstructions and cranial capacities are reported for four key specimens from the *Paranthropus* clade. The brain morphology of *Australopithecus africanus* appears more human like than that of *Paranthropus* in terms of overall frontal and temporal lobe shape. These new data do not support the proposal that increased encephalization is a shared feature between *Paranthropus* and early *Homo*. Our findings are consistent with the hypothesis that *Australopithecus africanus* could have been ancestral to *Homo*, and have implications for assessing the tempo and mode of early hominid neurological and cognitive evolution.

Journal of Human Evolution (2000) **38,** 695–717
doi:10.1006/jhev.1999.0378
Available online at http://www.idealibrary.com on IDEAL®

Introduction

Much of what is known about hominid brain evolution has been learned from endocranial casts (endocasts) that reproduce details of the external morphology of the brain from the internal surface of the braincase. Because these endocasts are usually from fragmentary pieces of fossilized skulls, their missing parts must be reconstructed.

*To whom correspondence should be addressed.

0047–2484/00/050695+23$35.00/0

Discoveries such as KNM-WT 17000 (*P. aethiopicus*) and KNM-WT 17400 (*P. boisei*) (Leakey & Walker, 1988; Walker *et al.*, 1986; Brown *et al.*, 1993) provide evidence of previously unknown parts of the *Paranthropus* brain. Prior to these discoveries, *Paranthropus* endocasts were sometimes reconstructed using endocasts of *A. africanus* (e.g., Sts 5) as a model (see below). In this study we compare endocasts of *Paranthropus* (including *P. robustus*, *P. aethiopicus*, *P. boisei*) with those of *Australopithecus africanus* and identify, quantify, and interpret previously unknown differences in the frontal and temporal lobe morphology between these genera. In addition, we provide revised estimates for the mean cranial capacity of *Paranthropus*.

Materials and methods

Previously unknown parts of the cerebral cortex in *Paranthropus* were observed and measured on both the endocast of KNM-WT 17000 (*P. aethiopicus*) and on a silicone endocast prepared from a cast of KNM-WT 17400 (*P. boisei*). Corresponding observations and measurements for *Australopithecus africanus* were obtained from silicone endocasts prepared from museum casts of Sts 5 (Mrs. Ples) and Stw 505 (Mr. Ples), as well as from a copy of the natural endocast of Sts 60. Other endocasts used for comparative purposes included KNM-ER 23000 (*P. boisei*), Sts 19 (*A. africanus*) and the Sterkfontein Number 2 natural endocast (*A. africanus*). Comparative endocast measurements were taken (by JG) from ten gorillas (*G. gorilla*), nine chimpanzees (*P. troglodytes*), nine bonobos (*P. paniscus*), and ten modern humans. Associated cranial capacities were obtained with mustard seed for the gorilla and chimpanzee sample and from the literature for the human, bonobo, and early hominid sample.

As a preliminary step, GWW and DF validated the size of the silicone endocasts for two of the specimens (Sts 5 and Stw 505) by comparing several measurements obtained using calipers with measurements taken on their corresponding virtual endocasts that had been acquired with 3D-CT technology from the original skulls (Conroy *et al.*, 1998). The maximum length, height, and width obtained by measuring the virtual endocast of Sts 5 on the computer screen were 0·98, 1·00, and 1·00 of the respective measurements obtained with calipers from the silicone endocast. The length of the fragmentary Stw 505 virtual endocast and the distance between its left frontal and temporal poles were each 0·98 of the respective measurements obtained from the silicone endocast. A third measurement on the virtual endocast of Stw 505 (between its highest point on the dorsal surface and its lowest point at the anterior end of the temporal lobe) measured 0·99 of the comparable measurement of the silicone endocast. Thus, as detailed elsewhere (Weber *et al.*, 1998), endocasts prepared from museum quality casts of skulls reproduce measurements obtained with 3D-CT technology from the braincases of the original specimens with a high degree of accuracy.

Eight measurements (described below) were obtained with calipers from basal views of endocasts and projected onto the basal plane. The procedure for orienting an endocast in basal view is to first determine the maximum antero-posterior diameter of the endocast in left lateral view (using the right hemisphere, if left is not present) that connects the frontal and occipital poles as described and illustrated by Connolly (1950:124–125). The endocast is then turned upside down and secured so that the maximum anterior-posterior diameter is in the horizontal or basal plane and the mid-sagittal plane is vertical. In cases of partial endocasts (e.g., Sts 60, Stw 505; KNM-WT 17400), basal orientations were estimated by aligning them next to correctly oriented full endocasts from the same genus (e.g., Sts

5; KNM-WT 17000). The fossil hominid measurements were from undistorted and unreconstructed portions of endocasts. In order to reduce potential observer error or bias, measurements were taken together by three observers (DF, JG, and JCR) on two different occasions and the results averaged. JG took the measurements with sliding calipers, while JR and DF confirmed his selection of landmarks and readings from the calipers, and made sure the calipers remained oriented so that measurements were projected onto the basal plane.

In order to quantify remeasurement error, the three workers together repeated all of the measurements on the fossil hominids one year after the first measurements were obtained and then compared their results with the earlier ones. For each of the eight measurements, remeasurement error was calculated as the mean of the absolute differences (determined for each specimen) between the first and second sets of measurements. Remeasurement error was then expressed as a percentage of the average length for each measurement. The results were 1% for measurements 1, 2, 6, and 8; and ranged from 2–8% for the other four measurements. The highest remeasurement errors expressed as percentages of mean lengths were for the shortest lengths. Similarly, JG remeasured 12 endocasts (three each from humans, bonobos, chimpanzees, and gorillas) one year after taking the initial measurements from these specimens. The results ranged from 1–8%, with the greatest relative remeasurement error associated with the shortest lengths.

The measurements included (Figure 1): (1) **bat–bat**, the distance between the most anterior points of the temporal lobes in basal view; (2) **mat–mat**, maximum width of the frontal lobes at the level of **bat**; (3) **mbat–rof(tan)**, the shortest distance between the middle of the line connecting the two **bats** and the tangent to the most rostral point on the orbital surfaces of the frontal lobes (note that **rof** should not be confused with the frontal pole); (4) **mcp–mbat**, the shortest distance between the middle clinoid process (or anterior border of the sella turcica) and **mbat**; (5) **mcp–rof(tan)**, the shortest distance between the middle clinoid process and **rof(tan)**; (6) **cob–rof(tan)**, the shortest distance between the caudal boundary of the olfactory bulbs (cribriform plate) and **rof(tan)**; (7) **rob–rof(tan)**, the shortest distance between the rostral boundary of the olfactory bulbs and **rof(tan)**; (8) **rof(tan)–bpc(tan)**, the shortest distance between **rof(tan)** and the tangent to the most

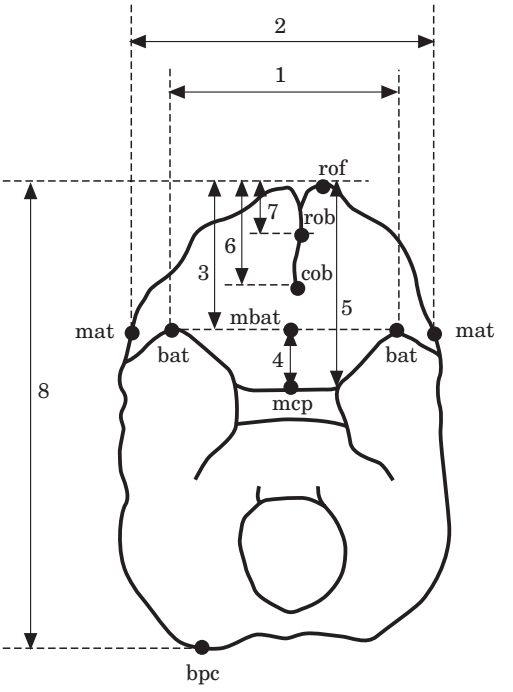

Figure 1. Measurements obtained from basal views and projected onto the horizontal (basal) plane from endocasts of australopithecines, apes, and humans (see text for details and Table 1 for data). Landmarks: **bat**, most anterior point on temporal lobe from basal view; **mat**, most lateral point on endocast at the level of **bat** in basal plane; **mbat**; middle of the line connecting the two **bats**; **rof**, the most rostral point on the orbital surfaces of the frontal lobes; **mcp**, middle clinoid process; **cob**, caudal boundary of olfactory bulbs (cribriform plate) in midline; **rob**, rostral boundary of olfactory bulbs in midline; **bpc**, most posterior point on cerebella in basal view.

posterior point on the cerebella in basal view (**bpc**).

Measurements 3, 6, 7, and 8 were used to calculate three additional lengths for each specimen: [3–6] the length between **mbat** and **cob**; [6–7], the length of the olfactory bulb (cribriform plate); and [8–3], the length of the basal aspect of the endocast caudal to **mbat**. Indices that express each measure as a percentage of endocast length in basal view were calculated by dividing these three lengths as well as measurements 1–7 by measurement 8 for the great ape and human samples, and for the two hominid endocasts for which measurement 8 was available (KNM-WT 17000 and Sts 5).

Descriptive statistics were provided for the lengths (Table 1) and indices (Table 2) obtained from endocasts of *Homo*, *Gorilla*, *Pan*, *Paranthropus* and *Australopithecus*. These data were first compared in living hominoids in order to establish a comparative basis for assessing endocasts representing *Australopithecus* and *Paranthropus*. For all of the comparisons in this study, there were significant differences between groups which were determined by post-hoc analyses of selected contrast within the general linear model (GLM) of *SPSS* (version 8.0). The alpha level was preset to $P \leq 0{\cdot}05$ after correction with Bonferroni's method for multiple comparisons where the indicated *P*-values had been adjusted (Tables 2 & 3). Differences in the mean lengths and indices were also tested for statistical significance between the two species of *Pan*. The only two measurements that were found to differ significantly between *P. troglodytes* and *P. paniscus* were variables 4 and 4/8. Consequently, for these two variables, results are reported separately for these two species. Endocasts of *Paranthropus* and *Australopithecus* were compared to each other and to endocasts from *Pan*, *Gorilla*, and *Homo* (Table 3) by computing mean differences, standard errors, and *P*-values from the data provided in Table 1. Finally, the above observations and statistically significant results were synthesized and the key features summarized for endocasts from apes, early hominids, and humans (Table 4).

Additionally, because previously unknown parts of *Paranthropus* endocasts are now available, new endocast reconstructions were made for *Paranthropus* specimens SK 1585 (*P. robustus*), OH 5 (*P. boisei*), KNM-ER 732 (*P. boisei*), and KNM-ER 407 (*P. boisei*), using appropriate *unreconstructed* parts of *Paranthropus* endocasts as models. Endocast reconstruction methods and cranial capacity determinations are detailed in the Appendix.

Results

Gorilla, Pan, *and* Homo

Mean measurements from basal views of endocasts are presented in Table 1, and means of indices generated by dividing variables 1–7 and [3–6], [6–7] and [8–3] by endocast lengths are provided in Table 2. Not surprisingly, the means for larger-brained *Homo* are significantly greater than the means for smaller-brained *Gorilla* and *Pan* for variables 1–8, [6–7], and [8–3]. All *P*-values are $<0{\cdot}001$ except for the *Homo-Gorilla* comparison for variable 3 ($P=0{\cdot}021$). Variable [3–6], on the other hand, is significantly shorter in *Homo* than in *Gorilla* or *Pan* ($P<0{\cdot}001$), which corresponds with an increased mean length of variable 4 in *Homo* (indicating a greater extent of temporal pole projection, see below). *Gorilla* is significantly longer than *Pan* for variables 8 (endocast length) and [8–3] ($P<0{\cdot}001$ for both comparisons). For variable 4, on the other hand, *P. troglodytes* is significantly longer than *Gorilla* ($P<0{\cdot}001$) and *P. paniscus* ($P<0{\cdot}01$), which do not differ significantly from each other ($P=0{\cdot}82$).

The mean indices (Table 2) that express variables as percentages of endocast lengths

Table 1 Endocast measurements

	bat–bat 1	mat–mat 2	mbat–rof(tan) 3	mcp–mbat 4	mcp–rof(tan) 5	cob–rof(tan) 6	rob–rof(tan) 7	rof(tan) bpc(tan) 8	Cranial capacity (cm^3) 9	Length mbat–cob [3–6]	Length olf. bulb [6–7]	Base–caudal to bat [8–3]
Homo (n=10)												
Mean	69·70	108·90	38·90	16·00	53·89	30·30	9·00	150·10	1350	8·60	21·30	111·20
S.D.	6·27	7·42	3·76	2·31	5·88	4·74	2·11	6·71	175·50	3·92	4·52	6·61
Range	(58·0–80·0)	(98·0–121·0)	(34·0–43·0)	(12·0–20·0)	(46·0–64·0)	(22·0–37·0)	(6·0–12·0)	(140·0–164·0)	—	(1·0–13·0)	(14·0–27·0)	(101·0–122·0)
Gorilla (n=10)												
Mean	49·00	77·60	34·00	5·70	40·90	16·60	4·60	120·90	483·50	17·40	12·00	86·90
S.D.	2·49	4·62	2·91	1·77	3·25	1·90	1·51	5·90	79·33	2·27	0·67	5·26
Range	(45·0–52·0)	(71·0–86·0)	(31·0–39·0)	(3·0–8·0)	(37·0–46·0)	(13·0–19·0)	(2·0–7·0)	(114·0–129·0)	(375·0–585·0)	(13·0–20·0)	(11·0–13·0)	(80·0–96·0)
Pan (n=18)												
Mean	47·30	74·94	31·41	8·56	40·29	16·44	4·79	107·56	392·67	14·76	11·26	76·33
S.D.	3·66	5·22	3·17	2·23	3·99	2·93	1·35	3·88	25·00	2·70	3·54	4·68
Range	(40·0–53·0)	(64·0–83·0)	(26·0–36·0)	(5·0–12·0)	(32·0–45·0)	(10·0–21·0)	(2·0–8·0)	(97·0–114·0)	(360·0–445·0)	(10·0–22·0)	(1·0–17·0)	(66·0–84·0)
Paranthropus												
WT 17000	50·00	74·00	34·00	5·00	39·00	20·00	7·00	114·00	410·00	14·00	13·00	80·00
WT 17400	45·00	68·00	29·00	4·00	33·00	14·00	7·00	—	390·00	15·00	7·00	—
Mean	47·50	71·00	31·50	4·50	36·00	17·00	7·00	—	400·00	14·50	10·00	80·00
S.D.	3·54	4·24	3·54	0·71	4·24	4·24	0·00	—	14·14	0·71	4·24	—
Range	(45·0–50·0)	(68·0–74·0)	(29·0–34·0)	(4·0–5·0)	(33·0–39·0)	(14·0–20·0)	(7·0–7·0)	—	(390·0–410·0)	(14·0–15·0)	(7·0–13·0)	—
Australopithecus												
Sts 5	56·00	85·00	39·00	14·00	53·00	30·00	14·00	118·00	485·00	9·00	16·00	79·00
Stw 505	—	—	33·00	11·00	44·00	29·00	11·00	—	515·00	4·00	18·00	—
Sts 60	62·00	—	31·00	11·00	42·00	—	—	—	428·00	—	—	—
Mean	59·00	—	34·33	12·00	46·33	29·50	12·50	—	476·00	6·50	17·00	—
S.D.	4·24	—	4·16	1·73	5·86	0·71	2·12	—	44·19	2·50	1·00	—
Range	(56·0–62·0)	—	(31·0–39·0)	(11·0–14·0)	(42·0–53·0)	(29·0–30·0)	(11·0–14·0)	—	(428·0–515·0)	(4·0–9·0)	(16·0–18·0)	—

Note: Descriptive statistics for measurements (see Fig. 1) taken from endocasts of australopithecines, apes, and humans. Cranial capacities for gorillas and *Pan* were obtained from skulls, while those for humans are from Pakkenberg & Gundersen, 1997. Although the mean cranial capacity listed for *Pan* is for *P. troglodytes* only, a mean cranial capacity of 350 cm^3 has been published elsewhere for *P. paniscus* (Cramer, 1977). For Stw 505, **mbat** was determined by the intersection of the tangent to the left **bat** with the intact midsagittal plane.

Table 2 Descriptive statistics and *P*-values for endocast indices

	1/8	2/8	3/8	4/8	5/8	6/8	7/8	[3–6]/8	[6–7]/8	[8–3]/8
Homo (n=10)										
Mean	0·46*	0·73*	0·26†	0·11*†	0·36	0·20*†	0·06*†	0·06*†	0·14*†	0·74†
S.D.	0·04	0·03	0·02	0·02	0·04	0·03	0·01	0·03	0·03	0·02
Range	(0·38–0·50)	(0·66–0·76)	(0·22–0·30)	(0·08–0·13)	(0·31–0·42)	(0·16–0·25)	(0·04–0·08)	(0·01–0·09)	(0·10–0·18)	(0·70–0·78)
Gorilla (n=10)										
Mean	0·41*‡	0·64*‡	0·28	0·05*‡	0·34‡	0·14*	0·04*	0·14*	0·10*	0·72
S.D.	0·02	0·03	0·02	0·01	0·02	0·02	0·01	0·02	0·008	0·02
Range	(0·37–0·44)	(0·57–0·69)	(0·25–0·31)	(0·03–0·06)	(0·30–0·60)	(0·10–0·16)	(0·02–0·06)	(0·11–0·17)	(0·09–0·11)	(0·69–0·75)
Pan (n=18)										
Mean	0·44‡	0·69‡	0·29†	0·08†‡	0·37‡	0·15†	0·04†	0·14†	0·10†	0·71†
S.D.	0·03	0·04	0·03	0·02	0·04	0·03	0·01	0·02	0·03	0·03
Range	(0·38–0·49)	(0·62–0·77)	(0·25–0·34)	(0·05–0·11)	(0·30–0·42)	(0·09–0·20)	(0·02–0·08)	(0·01–0·20)	(0·01–0·16)	(0·66–0·75)
	*P<0·001	*P<0·001	†P=0·022	*P<0·001	‡P=0·04	*P<0·001	*P=0·001	*P<0·001	*P=0·004	†P=0·18
	‡P=0·026	‡P=0·003		†P=0·001		†P<0·001	†P=0·008	†P<0·001	†P=0·005	
				‡P<0·001						
Paranthropus										
KNM-WT 17000	0·44	0·65	0·30	0·04	0·34	0·18	0·06	0·12	0·11	0·70
Australopithecus										
Sts 5	0·47	0·72	0·33	0·12	0·45	0·25	0·12	0·08	0·14	0·67

Notes: Symbols represent a significant difference between groups: **Homo–Gorilla*; †*Homo–Pan*; ‡*Gorilla–Pan*.
Indices for endocasts in basal view were obtained by dividing the lengths of the variables provided in Table 1 by measurement 8. Significance tests were calculated with post-hoc multiple comparisons corrected with Bonferroni's method within the general linear model (type III) of SPSS. Indices were available for only one *Paranthropus* (KNM-WT 17000) and one *Australopithecus* (Sts 5) endocast. These are provided for comparative purposes, although they were not compared statistically with those of apes and humans.

in basal view indicate that *Gorilla* differs significantly from *Homo* and *Pan* in having generally narrower endocasts at the level of the temporal poles (variable 2/8, $P<0{\cdot}001$ and $P=0{\cdot}003$ respectively), temporal poles that are relatively closer together (variable 1/8, $P<0{\cdot}001$ and $P=0{\cdot}026$), and temporal poles that do not project as far forward relative to sella (variable 4/8, $P<0{\cdot}001$ for both comparisons). The mean relative lengths of the orbital surfaces of the frontal lobes of *Gorilla* (variable 5/8) are significantly shorter than those of *Pan* ($P=0{\cdot}04$), while the mean relative lengths of the two most anterior regions of the frontal lobes (variables 6/8 and 7/8, $P\leq 0{\cdot}001$ for both comparisons) and olfactory bulbs (variable [6–7]/8, $P=0{\cdot}004$) are significantly shorter than those of *Homo*.

Endocasts of *Pan*, on the other hand, are similar to those of *Homo* and differ significantly from those of *Gorilla* in mean relative width at the level of the temporal poles (variable 2/8), mean relative distance between the temporal poles (variable 1/8), and mean relative length of the frontal lobes (variable 5/8) ($P=0{\cdot}003$, $0{\cdot}026$, $0{\cdot}04$ respectively). The mean relative length of the portion of the frontal lobes that is anterior to the temporal poles (variable 3/8), however, is significantly longer in *Pan* than *Homo* ($P=0{\cdot}022$), but not *Gorilla*. Corresponding to this, the mean relative length of the posterior portion of the endocast (variable [8–3]/8) is significantly shorter in *Pan* than in *Homo* ($P=0{\cdot}018$). The mean relative projection of the temporal poles (variable 4/8) does not differ from that for *Homo* or *P. troglodytes* ($P=0{\cdot}63$), but is significantly shorter in *P. paniscus* than for both *Homo* ($P<0{\cdot}001$) and *P. troglodytes* ($P<0{\cdot}03$). This variable is significantly greater in *P. paniscus* ($P=0{\cdot}03$) and *P. troglodytes* ($P<0{\cdot}001$) than it is for *Gorilla*. As is the case for *Gorilla*, the mean relative lengths of the two most anterior regions of the frontal lobes (variables 6/8 and 7/8) and olfactory bulbs (variable [6–7]/8) of *Pan* are significantly shorter than those of *Homo* ($P<0{\cdot}001$, $0{\cdot}008$ and $0{\cdot}005$ respectively).

Although the mean relative length of the entire frontal lobe in basal view (variable 5/8) does not differ significantly between *Homo* and either of the two apes, the mean relative lengths of certain subregions within the frontal lobe (variables 6/8, 7/8, and [6–7]/8) are significantly longer in *Homo* than they are in *Gorilla* and *Pan* (see Table 2 for *P*-values). The mean relative length of variable 4/8 is also significantly longer in *Homo* than in *Gorilla* ($P<0{\cdot}001$) and *P. paniscus* ($P<0{\cdot}001$), but not *P. troglodytes*. On the other hand, the relative length between the anterior end of the temporal poles and the posterior end of the olfactory bulbs (variable [3–6]/8) is significantly shorter in *Homo* than in either ape ($P<0{\cdot}001$ for both comparisons). As detailed in the discussion section, these findings support other comparative studies on actual brains of apes and humans, which show that the frontal lobes of *Homo* are reorganized compared to those of *Gorilla* and *Pan*.

To summarize the main findings regarding the relative proportion of endocasts from living hominoids: endocasts of gorillas are generally longer and narrower than those of *Pan* (variables 8, [8–3], 1/8, and 2/8) and narrower than those of *Homo* (variables 1/8 and 2/8), while endocasts from *P. troglodytes* (but not *P. paniscus* or *Gorilla*) further resemble those of humans in having relatively projecting temporal poles (variable 4/8). Although the overall length of the human frontal lobe (variable 5/8) does not differ significantly from those of *Pan* or *Gorilla*, the proportions of areas *within* human frontal lobes are dramatically different from those of apes (variables 6/8, 7/8, [6–7]/8, [3–6]/8 and, except for *Pan troglodytes*, 4/8). In particular, the most anterior regions (variables 6 and 7) of the frontal lobe are relatively longer in humans.

Table 3 Mean difference, standard errors and *P*-values for comparisons with *Paranthropus* and *Australopithecus*

Comparison groups		Mean difference	Standard error	*P*-values
Group 1	Group 2			
Variable 1: bat–bat				
Paranthropus	*Pan*	0·20	3·13	1·000
	Gorilla	− 1·50	3·25	1·000
	Australopithecus	− 11·17	3·83	0·059
	Homo	− 22·20	3·25	<0·001*
Variable 2: mat–mat				
Paranthropus	*Pan*	− 3·94	4·25	1·000
	Gorilla	− 6·60	4·41	0·861
	Homo	− 37·90	4·41	<0·001*
Variable 3: mbat–rof(tan)				
Paranthropus	*Pan*	0·09	2·48	1·000
	Gorilla	− 2·50	2·58	1·000
	Australopithecus	− 2·83	3·04	1·000
	Homo	− 7·40	2·58	0·066
Variable 4: mcp–mbat				
Paranthropus	*Pan*	− 4·06	1·56	0·134
	Gorilla	− 1·20	1·62	1·000
	Australopithecus	− 7·50	1·91	0·004*
	Homo	− 11·50	1·62	<0·001*
Variable 5: mcp–rof(tan)				
Paranthropus	*Pan*	− 4·29	3·34	1·000
	Gorilla	− 4·90	3·47	1·000
	Australopithecus	− 10·33	4·09	0·158
	Homo	− 17·89	3·47	<0·001*
Variable 1: bat–bat				
Australopithecus	*Pan*	11·37	2·62	0·001*
	Gorilla	9·67	2·76	0·012*
	Homo	− 11·03	2·76	0·003*
Variable 2: mat–mat				
Australopithecus	*Pan*	—	—	—
	Gorilla	—	—	—
	Homo	—	—	—
Variable 3: mbat–rof(tan)				
Australopithecus	*Pan*	2·92	2·08	1·000
	Gorilla	0·33	2·19	1·000
	Homo	− 4·57	2·19	0·438
Variable 4: mcp–mbat				
Australopithecus	*Pan*	3·44	1·31	0·121
	Gorilla	6·30	1·38	0·001*
	Homo	− 4·00	1·38	0·062
Variable 5: mcp–rof(tan)				
Australopithecus	*Pan*	6·05	2·80	0·368
	Gorilla	5·43	2·95	0·733
	Homo	− 7·56	2·95	0·145

Table 3 (*Continued*)

Comparison groups		Mean difference	Standard error	*P*-values	Comparison groups		Mean difference	Standard error	*P*-values
Group 1	Group 2				Group 1	Group 2			
Variable 6: cob–rof(tan)					**Variable 6: cob–rof(tan)**				
Paranthropus	*Pan*	0·56	2·42	1·000	*Australopithecus*	*Pan*	13·06	2·02	<0·001*
	Gorilla	0·40	2·51	1·000		*Gorilla*	12·90	2·13	<0·001*
	Australopithecus	− 12·50	2·96	0·001*		*Homo*	− 0·80	2·13	1·000
	Homo	− 13·30	2·51	<0·001*					
Variable 7: rob–rof(tan)					**Variable 7: rob–rof(tan)**				
Paranthropus	*Pan*	2·21	1·18	0·696	*Australopithecus*	*Pan*	7·71	0·99	<0·001*
	Gorilla	2·40	1·23	0·583		*Gorilla*	7·90	1·05	<0·001*
	Australopithecus	− 5·50	1·45	0·005*		*Homo*	3·50	1·05	0·018*
	Homo	− 2·00	1·23	1·000					
Variable [3–6]: [mbat–cob]					**Variable [3–6]: [mbat–cob]**				
Paranthropus	*Pan*	− 0·26	2·17	1·000	*Australopithecus*	*Pan*	− 8·26	1·81	0·001*
	Gorilla	− 2·90	2·25	1·000		*Gorilla*	− 10·90	1·91	<0·001*
	Australopithecus	8·00	2·66	0·046*		*Homo*	− 2·10	1·91	1·000
	Homo	5·90	2·25	0·126					
Variable [6–7]: [cob–rof(tan)–rob–rof(tan)]					**Variable [6–7]: [cob–rof(tan)–rob–rof(tan)]**				
Paranthropus	*Pan*	− 1·26	2·45	1·000	*Australopithecus*	*Pan*	5·74	2·05	0·080
	Gorilla	− 2·00	2·55	1·000		*Gorilla*	5·00	2·16	0·264
	Australopithecus	− 7·00	3·00	0·251		*Homo*	− 4·30	2·16	0·541
	Homo	− 11·30	2·55	0·001*					

Endocasts for variables listed in Table 1. (*Pan* includes both *P. troglodytes* and *P. paniscus*.) Comparisons were done only for groups that contained two or more specimens for each variable, and significance tests were calculated with post-hoc multiple comparisons corrected with Bonferroni's method within the general linear model (type III) of SPSS (* indicates significant differences).

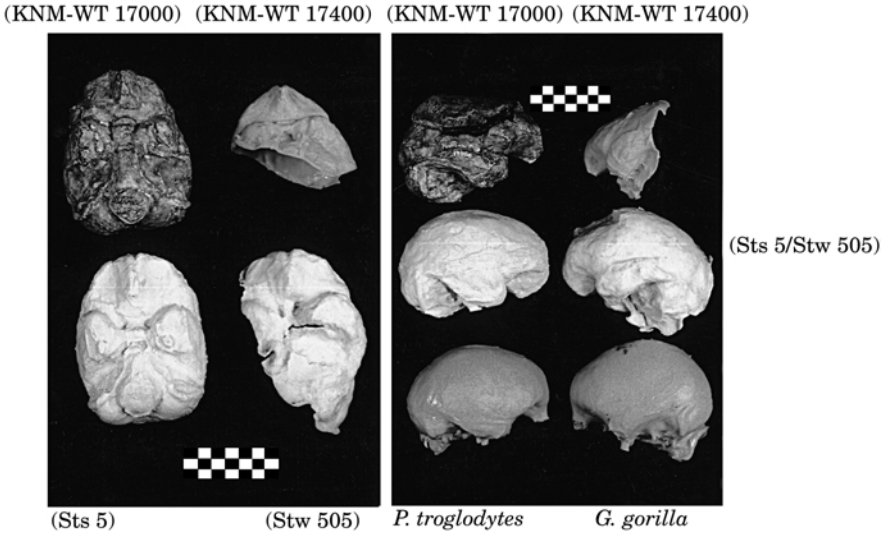

Figure 2. Basal (left) and lateral (right) views of endocasts from *A. africanus* specimens Sts 5 and Stw 505, and *Paranthropus* specimens KNM-WT 17000 and KNM-WT 17400. The lateral views are positioned frontal-lobe-to-frontal-lobe, and include a gorilla and chimpanzee for comparative purposes. Note the relatively expanded orbital surfaces of the frontal lobes of Sts 5 and Stw 505.

Paranthropus *and* Australopithecus

Table 3 presents mean differences, standard errors and *P*-values for comparisons of *Paranthropus* and *Australopithecus* with *Pan*, *Gorilla*, *Homo*, and each other for the variables in Table 1. As shown by the *P*-values, *Paranthropus* does not differ significantly from either *Pan* or *Gorilla* for any variable listed in Table 3. On the other hand, *Paranthropus* endocasts are significantly smaller than those of *Homo* for the means of variables 1, 2, 4, 5, 6, and [6–7] ($P \leq 0{\cdot}001$ for all six comparisons), which is not surprising given the much larger cranial capacity of the latter (Table 1). *Paranthropus* endocasts are also smaller than those of *Homo* for variables 3 and 7, although these comparisons do not reach statistical significance ($P = 0{\cdot}066$ and 1·0 respectively). Finally, *Paranthropus*, like both apes, is greater than *Homo* for variable [3–6], but not significantly so ($P = 0{\cdot}126$). These statistics reveal that endocasts of *Paranthropus* are entirely ape-like in the absolute variables that reflect the gross morphology of the frontal and temporal lobes of the brain. [It should be noted, however (see below), that KNM-WT 17000 differs from apes for indices 6/8 and 7/8.]

In lateral view, the ape like variables of the frontal lobes of *Paranthropus* are manifested in orbital surfaces that have a beaked-shaped profile similar to that of chimpanzees and gorillas (Figure 2), and unlike the more flattened orbital rostrum of humans. Viewed dorsally (Figure 3), the rostral portions of the frontal lobes in *Paranthropus* specimens KNM-WT 17000 and KNM-WT 17400 are relatively pointed (Holloway, 1988*b*), being comparable to the unreconstructed portions of OH 5 (*P. boisei*) and KNM-ER 23000 (*P. boisei*). These specimens show that the ape like variables for the frontal lobes that are reproduced from endocasts in our *Paranthropus* sample are manifested in an overall teardrop shape when viewed dorsally [Figure 3(b)]. Compared to endocasts from *Homo* and *Australopithecus* (see below), the ape like variables for the temporal lobes of *Paranthropus* are manifested in rounded temporal poles [KNM-WT 17000

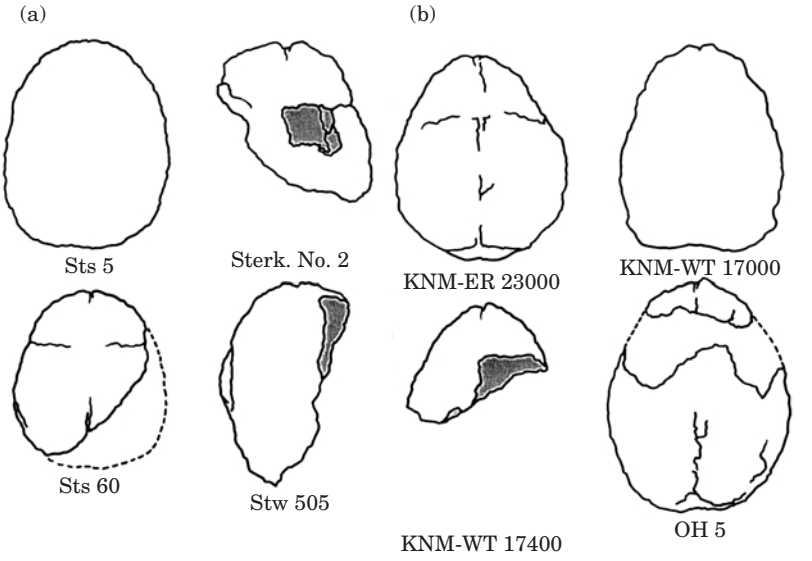

Figure 3. Outlines of dorsal views of endocasts from (a) *A. africanus* (Sts 5, Stw 505, Sts 60, No. 2 specimen from Sterkfontein), and (b) *Paranthropus* (OH 5, KNM-WT 17000, KNM-ER 23000, KNM-WT 17400). Endocasts of *Paranthropus* appear more pointed, while those of *A. africanus* are wider at the rostral ends of the frontal lobes.

(*P. aethiopicus*), KNM-WT 17400 (*P. boisei*), SK 1585 (*P. robustus*)], shorter forward projections of the poles beyond the anterior borders of sella turcica (variable 4, Table 3; Figure 2), and shorter distances between the temporal poles when seen in basal view (measurement 1, Table 3; Figure 2).

The picture for endocasts of *Australopithecus* is quite different. Despite the fact that mean cranial capacity of the *Australopithecus* specimens listed in Table 1 (476 cm^3) is between that of *Pan* (393 cm^3) and *Gorilla* (484 cm^3), a number of mean variables for *Australopithecus* are significantly larger than they are for either *Pan* or *Gorilla* (Table 3). These significant differences include variables 1 ($P=0{\cdot}001$ and $0{\cdot}012$ respectively), 6 ($P<0{\cdot}001$ for both comparisons), and 7 ($P<0{\cdot}001$ for both comparisons). For variable 4, *Australopithecus* is significantly larger than *Gorilla* and *P. paniscus* ($P=0{\cdot}001$ and $0{\cdot}003$ respectively), but not *P. troglodytes* ($P=1{\cdot}0$). On the other hand, *Australopithecus*, like *Homo*, is significantly smaller than both apes for variable [3–6] ($P\leq 0{\cdot}001$ for all four comparisons). In contrast to *Paranthropus*, and despite its small cranial capacity compared to *Homo*, endocasts of *Australopithecus* do not differ significantly from those of *Homo* for variables 4, 5, 6, and [6–7] (Table 3). Furthermore, variables 4, 6, and 7 are significantly larger in *Australopithecus* than in *Paranthropus* endocasts ($P=0{\cdot}004$, $0{\cdot}001$, and $0{\cdot}005$ respectively), while variable [3–6] is significantly smaller ($P<0{\cdot}05$).

The similarities between endocasts of *Australopithecus* and *Homo* are manifested in expanded and blunted, rather than beak-shaped, orbital rostra compared to apes and *Paranthropus* (variable 6, Tables 1 and 3; Figure 2), as well as cribriform plates (olfactory bulbs) that are longer on average (variable [6–7]). In *Australopithecus*, expansion of the frontal lobes in the region directly lateral to **rof** also produces a wider rostral end of the frontal lobe when viewed dorsally

compared to that seen in *Paranthropus* (Figure 3). Compared to *Paranthropus*, endocasts of *Australopithecus*, like those from *Homo*, also have temporal poles that project more in an anterior and lateral direction relative to sella turcica (variables 4 and 1, Tables 1 and 3; Figure 2).

Because endocast indices can be obtained for only one *Paranthropus* (KNM-WT 17000) and one *Australopithecus* endocast (Sts 5) (Table 2), comparisons of these indices for the two genera cannot be statistically analyzed as was done for the variables presented in Table 1. One may note, however, that the *Paranthropus* endocast falls on or nearer the ape means while the *Australopithecus* endocast falls on or nearer the *Homo* means for relative variables 1/8, 2/8, 4/8, [3–6]/8, and [6–7]/8 (Table 2). Interestingly, the *Australopithecus* endocast is noticeably larger than those for *Paranthropus*, *Homo*, and both apes for relative variables 3/8, 5/8, 6/8, and 7/8; and noticeably smaller for relative variable [8–3]/8 (Table 2).

Summary of key features on endocasts from Gorilla, Pan, Paranthropus, Australopithecus *and* Homo

The key findings regarding absolute and relative variables described above for endocasts of *Gorilla*, *Pan*, *Paranthropus*, *Australopithecus*, and *Homo* are summarized in Table 4. Except for the indices for *Paranthropus* and *Australopithecus* (and unless otherwise stated in the legend), table entries for *Homo* indicate that its mean differs significantly from the means for apes, while entries for apes indicate that their means differ significantly from those for the apes that are not marked. This table is conservative. For example, although the mean [6–7] for *Australopithecus* is intermediate between that of apes and *Homo* (Table 1), this variable is not marked because the differences between the mean for *Australopithecus* and those for apes did not achieve statistical significance (Table 3). Conversely, the indices for *Paranthropus* and *Australopithecus*, could not be compared statistically with means from other groups because they are available for only one specimen each (i.e., KNM-WT 17000 and Sts 5). In these cases, entries indicate whether the index measured from one representative is closer to that for apes (G and/or P) or humans (H) (Table 2).

The observations in Table 4 are organized into four complexes, each of which contains interrelated (dependent) features. With regards to general size and shape of endocasts, the long (variable 8) and narrow (1/8 and 2/8) endocasts of *Gorilla* differ markedly compared to those of *Pan*. Endocasts of *Homo*, however, are associated with larger cranial capacities than those of apes, as well as longer relative lengths of the posterior portion of the brain [8–3]/8 compared to *Pan*. Two indices for *Australopithecus* (5/8, [8–3]/8) differ noticeably from those of apes because variables 3 and 5 of Sts 5 are increased greatly compared to apes while its overall length (variable 8) is not. These indices are smaller in *Homo* than *Australopithecus*, on the other hand, because *Homo* equals Sts 5 in the mean dimensions of variables 3 and 5, but has a much longer mean overall length.

The second set of variables in Table 4 pertain to subdivisions on the orbital surfaces of the frontal lobes and reveal that *Australopithecus* and *Homo* differ similarly in a number of key features compared to those of apes and *Paranthropus*. Again, the noticeably larger indices for the frontal lobes of *Australopithecus* compared to *Homo* (Table 2: 3/8, 6/8, and 7/8) are largely the result of a shorter variable 8 for Sts 5 than for *Homo*. These observations are consistent with the interpretation that, compared to endocasts from apes and *Paranthropus*, endocasts of *Australopithecus* are characterized by differentially lengthened frontal lobes and subdivisions thereof, concomitantly with

Table 4 Summary of key endocast features for *Gorilla*, *Pan*, *Paranthropus*, *Australopithecus* and *Homo*

Description	Variable	*Gorilla*	*Pan*	*Paranthropus*	*Australopithecus*	*Homo*
General size and shape						
Cranial capacity	cm^3				+	
Absolute length endocast	8	+				+
Relative width bat–bat	1/8	−		*P*	*H*	$+^{G}$
Relative width mat–mat	2/8	−		*G*	*H*	$+^{G}$
Relative length mcp–rof	5/8		+	*G*	>*G*, *P*, *H*	
Absolute length mcp–rof	5					+
Relative length bpc–mbat	[8–3]/8			*P*	<*G*, *P*, *H*	$+^{Pan}$
Absolute length bpc–mbat	[8–3]	+				+
Frontal lobes						
Relative length mbat–rof	3/8			*P*	>*G*, *P*, *H*	$-^{Pan}$
Absolute length mbat–rof	3					+
Relative length mbat–cob	[3–6]/8			*G*, *P*	*H*	−
Absolute length mbat–cob	[3–6]				−	−
Relative length cob–rof	6/8			*H*	>*G*, *P*, *H*	+
Absolute length cob–rof	6				+	+
Relative length rob–rof	7/8			*H*	>*G*, *P*, *H*	+
Absolute length rob–rof	7				+	+
Olfactory bulbs						
Relative length cob–rob	[6–7]/8			*G*, *P*	*H*	+
Absolute length cob–rob	[6–7]					+
Temporal poles						
Relative length mcp–mbat	4/8		$+_{(P.\ troglodytes)}$	*G*	*H*	$+^{G,\ Pp}$
Absolute length mcp–mbat	4		$+_{(P.\ troglodytes)}$	$-^{Pt}$	$+^{G,\ Pp}$	+
Absolute width bat–bat	1				+	+

Based on statistical analyses of measurements obtained from basal views and illustrated in Figure 1. Symbols: + under *Homo* or *Australopithecus*, the mean for that variable is significantly *larger* than the means for apes; + under *Gorilla* or *Pan*, the mean is significantly larger than those for the unmarked apes; + with superscripts (e.g., $+^{G,\ Pp}$), the mean is significantly larger than the means for only the apes indicated by the superscript (superscripts: *G*, *Gorilla*; *Pan*, chimpanzees and bonobos; *Pp*, *Pan paniscus*; *Pt*, *Pan troglodytes*); + (*P. troglodytes*), the mean variable is significantly longer in *P. troglodytes* than either *P. paniscus* or *Gorilla*; − with and without superscripts, the same conventions as above, except that the means are significantly *smaller* than those for apes. Because indices could not be compared statistically with means from other groups for *Paranthropus* (KNM-WT 17000) and *Australopithecus* (Sts 5), *G* and/or *P*, or *H* indicate that a particular index is closer to the mean for *Gorilla* and/or *Pan* or *Homo* (Table 2); >*G*, *P*, *H* indicates that the index for Sts 5 is noticeably greater than the indices for *Gorilla*, *Pan*, and *Homo*, while <*G*, *P*, *H* means that the index for Sts 5 is noticeably smaller. Note that *Paranthropus* is similar to *Homo* for only two indices, and that none of its mean absolute variables differ significantly from those of apes in the same direction (+ or −) as *Homo*. *Australopithecus*, on the other hand, is similar to *Homo* for five indices, and the means of four of its absolute variables differ significantly from those of all apes in the same direction as *Homo*. These data have implications for understanding the sequence in which cortical reorganization occurred during hominid brain evolution.

relatively shortened posterior portions ([8–3]/8). This accounts for the comparatively expanded and squared-off appearance of the orbital rostra in *Australopithecus* endocasts (Figures 2 and 3).

Because olfactory regions represent a phylogenetically older part of the brain than neocortical areas (Finlay & Darlington, 1995), the two measurements pertaining to the olfactory bulbs are placed in a third complex (Table 4). As detailed in the discussion section, *Australopithecus* appears more like humans than apes in the size and shape of its olfactory bulbs. This is also true for the temporal poles described by the fourth complex of variables (Table 4), as confirmed by visual observation of endocasts from *Australopithecus* and *Homo*

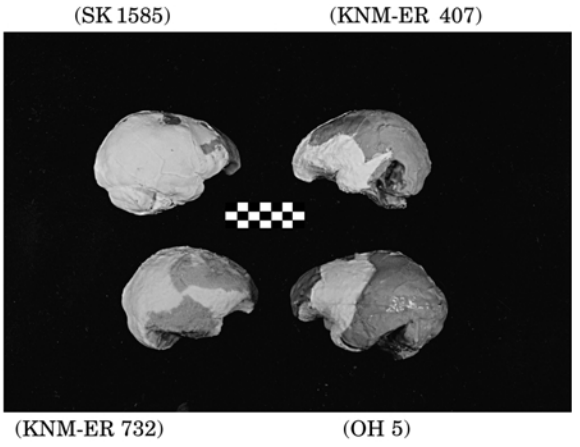

Figure 4. Newly reconstructed endocasts from four *Paranthropus* specimens. The reconstructed regions of SK 1585 are dark; those of KNM-ER 407, KNM-ER 732, and OH 5 are white. This endocast of SK 1585 contains matrix between the inferior border of the temporal lobe and the cerebellum that was removed in a subsequent procedure described in the Appendix. These reconstructions reproduce the beak-shaped rostral orbital area that is found in *Paranthropus*, but not *Australopithecus*.

that share a forward (4/8, 4) and lateral (1) projection of the temporal poles (Figure 2).

In sum, Table 4 reveals that endocasts of *Paranthropus* are similar to those of *Homo* for only two indices, while none of its mean absolute variables differ significantly from those of apes in the same direction (+ or −) as the means from endocasts of *Homo*. In contrast, endocasts of *Australopithecus* are similar to *Homo* endocasts for five indices, and the means of four of its absolute variables differ significantly from those of all apes in the same direction as the means from *Homo*. The implications of these data for understanding the sequence in which cortical reorganization occurred during hominid brain evolution are explored in the discussion section.

New endocranial capacities

Because much of the above information was not available when endocasts of *Paranthropus* specimens SK 1585, OH 5, KNM-ER 407, and KNM-ER 732 were reconstructed (apparently with the endocast of Sts 5 as a frequent model), we reconstructed the endocasts of these specimens (Figure 4), using the *unreconstructed* parts of other *Paranthropus* endocasts as models and recalculated their endocranial capacities (see Appendix for detailed descriptions of each reconstruction) (Table 5).

Five water displacements of the newly reconstructed endocast of SK 1585 (*P. robustus*) resulted in a mean of 476 cm^3 (470–484 cm^3), 54 cm^3 *less than* the currently accepted estimate of 530 cm^3 (Holloway, 1972) (Figure 4).

Five cranial capacity estimates of the newly reconstructed endocast of OH 5 (*P. boisei*) resulted in a mean of 500 cm^3 (498–502 cm^3), 30 cm^3 *less than* the currently accepted estimate of 530 cm^3 (Tobias, 1967) (Figure 4). This loss is due mostly to reduction in the orbital olfactory region compared to the earlier reconstruction, which did not benefit from reference to *Paranthropus* specimens that were discovered subsequent to its reconstruction. Our reconstruction differs from the earlier one in having a smaller, beaked-shaped rostral orbital region, and somewhat less anteriorly extended temporal poles (Holloway, 1972, 1975).

Five cranial capacity estimates for the newly reconstructed endocast of KNM-ER

Table 5 Cranial capacities for *Paranthropus* and *Australopithecus* specimens. Those for *A. africanus* are from the literature

Species	Dating (Ma)	Specimen	Cranial capacity (cm^3)	Reference	This study	Method	Eval.
P. robustus	~1·8–1·7	SK 1585	530	1	**476**	**B**	**1**
P. aethiopicus	~2·5	KNM-WT 17000	410	2	(410)		
P. boisei	~2·4	Omo L338y-6	427	3	(427)		
	~1·88	KNM-ER 13750	450–480 or 500	4 5	—		
	~1·9	KNM-ER 23000	491	5	(491)		
	~1·8	KNM-WT 17400	390–400 or 500	4 5	(390)		
	~1·8	OH 5	530	6	**500**	**A**	**1**
	~1·7	KNM-ER 406	525	7	—		
	~1·85	KNM-ER 407	510	7	**438**	**B**	**1–2**
	~1·7	KNM-ER 732	500	7	**466**	**B**	**1**
	~2·2	Omo 323	490	5	—		
		Mean	479·4 or 492·1		**449·8**		
A. africanus	~3·0	MLD 37/38	425	8			
	~3·0–2·5	Sts 60	428	7			
		Sts 71	428	9			
		Sts 5	485	7			
		Sts 19	436	7			
	~2·8–2·6	Stw 505	515	10			
	~2·5–1·0?	Taung	440	7			
		Mean	**451**				

Revised cranial capacities for *Paranthropus* are in bold; those that are accepted from the literature are in parentheses. The first mean for *Paranthropus* includes estimates for KNM-ER 13750 and KNM-WT 17400 from Holloway (1988*b*); the second mean uses estimates for these two specimens from Brown *et al.* (1993). Our acceptance of the estimate for Omo L338y-6 is tentative pending an opportunity to do our own reconstruction. KNM-ER 13750 is excluded from the present study because of the disparity in estimates between Holloway (1988*b*) and Brown *et al.* (1993) and the fact that we do not have a copy of this specimen from which to make our own judgment. We accept the lower estimate for KNM-WT 17400 from Holloway (1988*b*) after comparing this specimen with a large number of ape and australopithecine endocasts in our collection. KNM-ER 406 is excluded because its capacity is based on external skull measurements and calculated from a formula that incorporates a factor (f) that is based on erroneous cranial capacity estimates for OH 5 and SK 1585 (Holloway, 1973). Omo 323 is excluded because it is too fragmentary to yield an accurate estimate. References: **1**, Holloway (1972); **2**, Walker *et al.* (1986); **3**, Holloway (1981); **4**, Holloway (1988*b*); **5**, Brown *et al.* (1993); **6**, Tobias (1967); **7**, Holloway (1988*a*); **8**, Conroy *et al.* (1990); **9**, Conroy *et al.* (2000); **10**, Conroy *et al.* (1998). Methods: **A**, water displacement of a full or hemi-endocast (times two) reconstructed in silicone with minimal distortion; **B**, volume of water contained by mold of hemi-endocast times two. Evaluations of confidence in cranial capacity estimates due to completeness of original specimens: **1**, highest confidence; **2**, high confidence. See Appendix for details of the new endocast reconstructions.

732 (*P. boisei*) result in a mean of 466 cm^3 (460–472 cm^3), 34 cm^3 *less than* the currently accepted estimate of 500 cm^3 (Holloway, 1988*a*) (Figure 4). Our reconstruction differs from the earlier one in having a smaller, beaked-shaped rostral orbital region.

Five cranial capacity estimates for the newly reconstructed endocast of KNM-ER 407 (*P. boisei*) result in a mean of 438 cm^3 (430–446 cm^3), 72 cm^3 *less than* the currently accepted estimate of 510 cm^3 (Holloway, 1988*a*) and 68 cm^3 *less than* an earlier estimate of 506 cm^3 (Falk & Kasinga,

1983) (Figure 4). Our reconstruction differs from earlier ones in that most of the frontal lobe and temporal pole required reconstruction using the appropriate *Paranthropus* models.

Table 5 compares currently accepted endocranial capacities of *Paranthropus* with our revised values (estimates of other specimens in parentheses are considered acceptable). Our new estimates for these four *Paranthropus* specimens are all lower than earlier estimates, and the new mean of 450 cm^3 for eight specimens is significantly ($P<0{\cdot}05$, two-tailed) lower than one of the currently accepted means of 492 cm^3 (Table 5). However, the new mean does not differ significantly from that of 451 cm^3 for *Australopithecus* ($P\leq 0{\cdot}95$), which contradicts the commonly held view that *Paranthropus* and early *Homo* had, on average, significantly larger brains than *Australopithecus* (Holloway, 1973).

Discussion

The more human like cortical morphology reproduced on *Australopithecus* endocasts is not due to allometric scaling because (1) the mean endocranial volume of the three *Australopithecus* specimens measured in this study is less than that for both gorillas and humans (Table 1), and (2) because the mean endocranial volume of a wider sample of seven *Australopithecus* specimens does not differ significantly from that of eight *Paranthropus* specimens ($P\leq 0{\cdot}95$, Table 5). Furthermore, it is unlikely that the beak-shaped orbital rostra of endocasts from apes and *Paranthropus* are due to a high degree of postorbital constriction in their skulls, since skulls of *Australopithecus* that are also characterized by a high degree of postorbital constriction produce endocasts with orbital surfaces that are expanded and wide, rather than pointed (beak-shaped) and narrow at the very front (Figure 2). Thus, as others have suggested (Dean, 1988), endocranial aspects of the *cranial base*, while greatly influenced by the morphology of the brain, appear to be relatively independent from aspects of the masticatory system. It is also important to note that, although the cranial base of the skull has been shown to be affected by intentional deformation of the cranial vault (for cultural reasons) in native Americans, the effect is indirect via the altered cranial vault's effects on brain growth (Cheverud *et al.*, 1992; Kohn *et al.*, 1993). These studies show that the cranial base responds directly to changes in brain growth.

An extensive literature based largely on comparative studies of actual brains indicates that the enlarged brain of *Homo sapiens* is derived compared to the brains of extant apes (Connolly, 1950; Holloway, 1988*b*; Falk, 1992; Semendeferi, 1994; Deacon, 1997; Tobias, 1997; Passingham, 1998; Semendeferi & Damasio, 2000). Within this context, frontal lobes have traditionally been of special interest to paleoneurologists because of their known functions with respect to language, abstract thought, planning, and execution of motor activities. For example, comparative studies on actual brains led both Deacon (1997) and Semendeferi (1994) to conclude that prefrontal regions of the frontal lobes are enlarged and derived in humans as a result of cortical reorganization that occurred during the evolution of their early hominid ancestors. Passingham (1998) arrived at the same conclusion regarding the inferior frontal cortex and temporal lobe. It is also important to note that brains need not be enlarged to be derived, i.e., that neurological evolution may entail cortical reorganization or redistribution of cortical tissues without an increase in brain size (Holloway, 1988*b*). The developmental mechanisms that are likely to have operated during the course of brain expansion and reorganization in mammals, including humans, have recently been elucidated within a framework that

accommodates both allometric scaling and the evolution of neurological specializations (Finlay & Darlington, 1995).

Holloway's (1975, 1988*b*) longheld belief that cortical reorganization may already have been underway in australopithecines prior to the increase in brain size that occurred subsequently in *Homo* is supported by our observations for *Australopithecus*, but not *Paranthropus*. As detailed below, our morphological findings for the orbital surfaces of *Australopithecus* endocasts correspond with the reorganized cortical morphology that Semendeferi (1994) earlier hypothesized would have existed in the hominid ancestors of *Homo* and that would have been derived relative to the more primitive ape like morphology. Specifically, our analysis of endocasts has shown that the orbital surfaces of the frontal lobes of *Australopithecus* were expanded and the relative lengths of subareas rearranged (reorganized) compared to *Paranthropus*, which appears more ape like and less human like than *Australopithecus*.

Some phylogenetic speculations

Using *Australopithecus* as a hypothetical model for the ancestral *Homo* condition, it is possible to hypothesize about the sequence in which certain neurological features reorganized during the course of hominid evolution. It thus appears that the frontal lobes and temporal poles may have increased in size early on (i.e., in the australopithecine ancestors of *Homo*), followed by subsequent (additional) enlargement of posterior regions during the course of brain evolution in *Homo*. In addition to an increase in overall size of the frontal lobes (as indicated by length), the subregions within the orbital surfaces of the frontal lobes appear to have become reorganized with respect to one another in a sequential manner. For example, although human olfactory bulbs are estimated to be roughly 1/2 to 1/3 the volume of those of *P. troglodytes* and *Gorilla gorilla* (Stephan *et al.*, 1981), inspection of endocasts shows that the shape of the human olfactory bulb is long and flattened compared to the shorter, more protuberant bulbs of apes. In keeping with this, the olfactory bulb measurement [6–7] of 21 mm is longer in humans than in apes and *Paranthropus* (Table 1). Measurement 6 (the length of the olfactory bulb plus measurement 7) averages 30 mm in both *Australopithecus* and humans. However, the mean length of the olfactory bulb in *Australopithecus* (17 mm) is 4 mm shorter than the mean for humans, while that of measurement 7 is 3·5 mm longer. These differences would disappear if the olfactory bulbs increased their length rostrally by 4 mm—i.e., to the human length while maintaining the overall length of measurement 6. These data are consistent with the hypothesis that the orbital surface of the frontal lobes was expanded in the region of **rof** in conjunction with some lengthening and flattening of the olfactory bulbs in *Australopithecus* compared to *Paranthropus*, and that the olfactory bulbs continued to lengthen in a rostral direction subsequent to this (i.e., in descendants of *Australopithecus* that may have given rise to *Homo*).

Our findings have wider implications for the evolution of cognition in early hominids. Both the blunt-shaped, relatively enlarged portions of the orbital surfaces of the frontal lobes and the anteriorly expanded, laterally pointed temporal poles of *Australopithecus* appear more human like compared to *Paranthropus* and African apes. The area that is expanded near **rof** in the frontal lobes of *Australopithecus* corresponds to Brodmann's area 10 in both apes and humans, which has been shown experimentally to be involved in abstract thinking, planning of future actions, and undertaking initiatives (Semendeferi, 1994). Because the relative size of human area 10 is twice that of both bonobos and chimpanzees, Semendeferi (1994) suggested that this area of the cerebral cortex increased

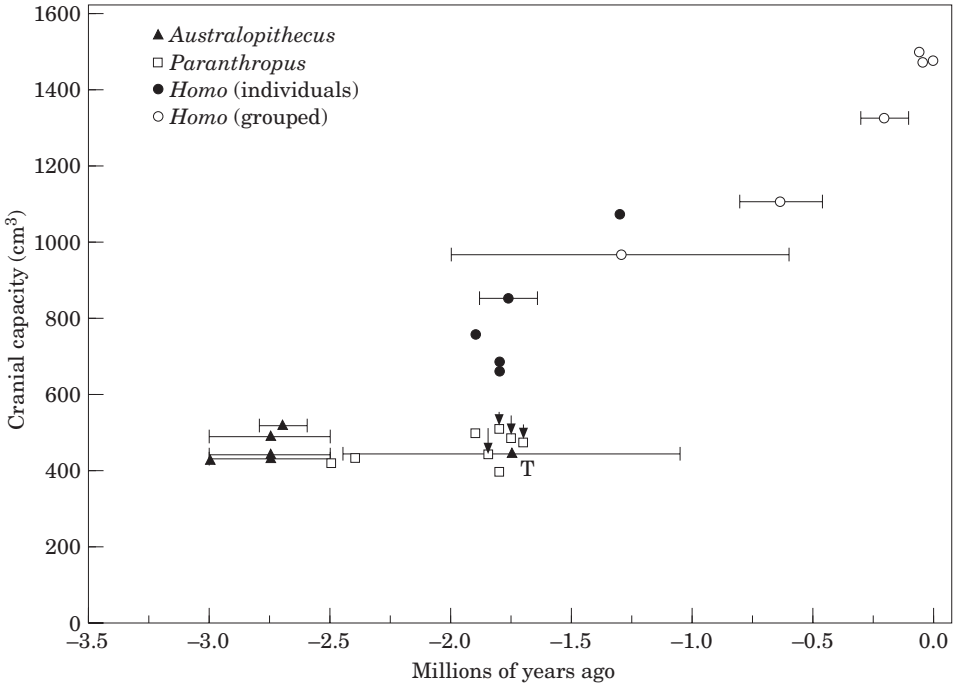

Figure 5. Cranial capacities from *Australopithecus* and *Paranthropus* plotted against time (Table 5). For comparative purposes, cranial capacities are also provided for a number of key representatives of *Homo* (both individuals and groups; see Falk, 1987 for data). The relative dates for the South African specimens are indicated by error bars; the East African specimens (all *Paranthropus*) are associated with more precise radiometric dates. The age estimates for Taung are from Partridge (1986) and McKee (1993). The error bars for the dates for *Homo* provide the general range of dates that have been suggested by various workers for individuals or groups (Falk, 1987; Swisher *et al.*, 1994). The four arrows illustrate the magnitude of the decrease in new cranial capacities reported on here compared to earlier estimates. **T** indicates the adult projection for Taung, which is the only hominid from its site and, although it is the type specimen for *A. africanus*, manifests a number of *Paranthropus*-like characteristics in its skull, teeth, and endocast (Falk *et al.*, 1995). This graph and the morphological data pertaining to endocasts (see text) suggest that brain size may have begun to increase in australopithecine ancestors of *Homo* between 2·5 and 3·0 Ma.

in relative size at some point along the line from the first hominids to the early representatives of the genus *Homo*. Our results support her suggestion, and further suggest that area 10 had begun to increase in size in *Australopithecus*.

Significantly, the temporal poles of chimpanzees (area TG) receive fibers from the orbital surface of the frontal lobe (area FF) (Bailey *et al.*, 1950). In humans, the temporal poles (Brodmann's area 38) connect with the frontal lobes, limbic structures, and

> "through their interconnections with visual and auditory association cortex, an elaborate association complex is built up in this anterior end of the temporal lobe"

(Crosby *et al.*, 1962:472). Interestingly, the anterior lateral regions of the temporal poles of humans are activated during the recognition and naming of familiar human faces (Damasio *et al.*, 1996).

Until now, received wisdom has been that brain size began to increase rapidly in the genus *Homo* around 2·0 Ma (Falk, 1992). Our findings that *Paranthropus* had smaller average cranial capacities than previously believed (Conroy *et al.*, 1998; Falk, 1998), and that reorganization of the frontal and

temporal lobes appears to have been underway in *Australopithecus* well before 2·0 Ma, suggest that the trends for increased brain size and cortical reorganization may have begun one million years earlier than previously believed—i.e., in the *Australopithecus* ancestors of *Homo* (Figure 5). Evidence pertaining to cranial blood flow, on the other hand, suggests that earlier hominid species, like *A. afarensis* from Hadar, Ethiopia (now placed in the genus *Praeanthropus* by Strait *et al.*, 1997) could have been ancestral to *Paranthropus*, but not to the *Australopithecus–Homo* lineage (Falk & Conroy, 1983; Falk *et al.*, 1995; Falk & Gage, 1998). These hypotheses are consistent with the recent findings of other workers based on analyses of postcrania (Berger, 1998; McHenry & Berger, 1998). As additional fossil hominids come to light, we look forward to learning more about wider areas of the cerebral cortex in early hominids, and to future tests of the ideas and hypotheses presented in this paper.

Acknowledgements

This research is supported by NSF grant SBR-9729796 (DF), and was made possible by the cooperation of curators at the Transvaal Museum in Pretoria (C. K. Brain and E. Vrba), the Department of Anatomy at the University of Witwatersrand in Johannesburg (P. V. Tobias), and the National Museums of Kenya (R. Leakey) who generously provided DF with casts and endocasts from original specimens. We thank Tim Gage and Bruce Dudek for statistical advice, Dieter zur Nedden for making his CT unit available to us, Alan Walker for helping us to obtain copies of hominid endocasts and for providing a copy of the occipital endocast of Omo L338y-6, R. MacPhee and F. Brady for permitting us to make endocasts from ape skulls at the American Museum of Natural History, and Terry Harrison for helpful suggestions regarding the manuscript.

References

Bailey, P., Bonin, G. von & McCulloch, W. S. (1950). *The Isocortex of the Chimpanzee*. Urbana: University of Illinois Press.

Berger, L. R. (1998). The dawn of humans, redrawing our family tree? *Nat. Geog.* **194,** 90–99.

Brown, B., Walker, A., Ward, C. V. & Leakey, R. E. (1993). New *Australopithecus boisei* calvaria from east Lake Turkana. *Am. J. phys. Anthrop.* **91,** 137–159.

Cheverud, J., Kohn, L. A. P., Konigsberg, L. W. & Leigh, S. R. (1992). Effects of fronto-occipital artificial cranial vault modification on the cranial base and face. *Am. J. phys. Anthrop.* **88,** 323–345.

Connolly, J. C. (1950). *External Morphology of the Primate Brain*. Springfield, Illinois: Charles C. Thomas.

Conroy, G. C., Falk, D., Guyer, J., Weber, G., Seidler, H. & Recheis, W. (2000). Endocranial capacity in Sts 71 (*Australopithecus africanus*). *Anat. Rec.* in press.

Conroy, G. C., Vannier, M. W. & Tobias, P. V. (1990). Endocranial features of *Australopithecus africanus* revealed by 2- and 3-D computed tomography. *Science* **247,** 838–841.

Conroy, G. C., Weber, G. W., Seidler, H., Tobias, P. V., Kane, A. & Brunsden, B. (1998). Endocranial capacity in an early hominid cranium from Sterkfontein, South Africa. *Science* **280,** 1730–1731.

Cramer, D. L. (1977). Craniofacial morphology of *P. paniscus*: a morphometric and evolutionary appraisal. *Contrib. Primatol.* **10,** 1–64.

Crosby, E. C., Humphrey, T. & Lauer, E. W. (1962). *Correlative Anatomy of the Nervous System*. New York: Macmillan.

Damasio, H., Grabowski, T. J., Tranel, D., Hichwa, R. D. & Damasio, A. R. (1996). A neural basis for lexical retrieval. *Nature* **380,** 499–505.

Deacon, T. W. (1997). *The Symbolic Species*. New York: W. W. Norton.

Dean, M. C. (1988). Growth processes in the cranial base of hominoids and their bearing on morphological similarities that exist in the cranial base of *Homo* and *Paranthropus*. In (F. Grine, Ed.) *Evolutionary History of the "Robust" Australopithecines*, pp. 107–112. New York: Aldine de Gruyter.

Falk, D. (1983). Cerebral cortices of East African early hominids. *Science* **221,** 1072–1074.

Falk, D. (1987). Hominid paleoneurology. *Ann. Rev. Anthrop.* **16,** 13–30.

Falk, D. (1992). *Evolution of the Brain and Cognition in Hominids* (James Arthur Lecture). New York: American Museum of Natural History.

Falk, D. (1998). Hominid brain evolution: looks can be deceiving. *Science* **280,** 1714.

Falk, D. & Conroy, G. C. (1983). The cranial venous sinus system in *Australopithecus afarensis*. *Nature* **306,** 779–781.

Falk, D. & Gage, T. (1998). Radiators are cool: a response to Braga & Boesch's published paper and reply. *J. hum. Evol.* **35,** 307–312.
Falk, D. & Kasinga, S. (1983). Cranial capacity of a female robust australopithecine (KNM-ER 407) from Kenya. *J. hum. Evol.* **12,** 515–518.
Falk, D., Gage, T. B., Dudek, B. & Olson, T. R. (1995). Did more than one species of hominid coexist before 3·0 ma?: evidence from blood and teeth. *J. hum. Evol.* **29,** 591–600.
Finlay, B. L. & Darlington, R. B. (1995). Linked regularities in the development and evolution of mammalian brains. *Science* **268,** 1578–1584.
Holloway, R. L. (1972). New australopithecine endocast, SK 1585, from Swartkrans, South Africa. *Am. J. phys. Anthrop.* **37,** 173–186.
Holloway, R. L. (1973). New endocranial values for the East African early hominids. *Nature* **243,** 97–99.
Holloway, R. L. (1975). Early hominid endocasts: volumes, morphology and significance for hominid evolution. In (R. H. Tuttle, Ed.) *Primate Functional Morphology and Evolution*, pp. 391–415. The Hague: Mouton.
Holloway, R. L. (1981). The endocast of the Omo juvenile L338y-6 hominid specimen. *Am. J. phys. Anthrop.* **54,** 109–118.
Holloway, R. L. (1983). Human paleontological evidence relevant to language behavior. *Hum. Neurobiol.* **2,** 105–114.
Holloway, R. L. (1988*a*). Brain. In (I. Tattersall, E. Delson & J. van Couvering, Eds) *Encyclopedia of Human Evolution and Prehistory*, pp. 98–105. New York: Garland.
Holloway, R. L. (1988*b*). "Robust" australopithecine brain endocasts: some preliminary observations. In (F. Grine, Ed.) *Evolutionary History of the "Robust" Australopithecines*, pp. 97–105. New York: Aldine de Gruyter.
Kohn, L. A. P., Leigh, S., Jacobs, S. & Cheverud, J. (1993). Effects of annular cranial vault modification on the cranial base and face. *Am. J. phys. Anthrop.* **90,** 147–168.
Leakey, R. E. F. & Walker, A. (1988). New *Australopithecus boisei* specimens from east and west Lake Turkana. *Am. J. phys. Anthrop.* **76,** 1–24.
McHenry, H. M. & Berger, L. R. (1998). Body proportions in *Australopithecus afarensis* and *A. africanus* and the origin of the genus *Homo*. *J. hum. Evol.* **35,** 1–22.
McKee, J. K. (1993). Faunal dating of the Taung hominid fossil deposit. *J. hum. Evol.* **25,** 363–376.
Pakkenberg, B. & Gundersen, J. G. (1997). Neocortical neuron number in humans: effect of sex and age. *J. Comp. Neurol.* **384,** 312–320.
Partridge, T. (1986). Paleoecology of the Pliocene and lower Pleistocene hominids of southern Africa: how good is the chronological and paleoenvironmental evidence? *S. Afr. J. Sci.* **82,** 80–83.
Passingham, R. E. (1998). The specializations of the human neocortex. In (A. D. Milner, Ed.) *Comparative Neuropsychology*, pp. 271–298. Oxford: Oxford University Press.
Semendeferi, K. (1994). Evolution of the hominoid prefrontal cortex: a quantitative and image analysis of area 13 and 10. Ph.D. Dissertation, University of Iowa.
Semendeferi, K. & Damasio, H. (2000). Brain size in living hominoids. *J. hum. Evol.* in press.
Stephan, H., Frahm, H. & Baron, G. (1981). New and revised data on volumes of brain structures in insectivores and primates. *Folia primatol.* **35,** 1–29.
Strait, D. S., Grine, F. E. & Moniz, M. A. (1997). A reappraisal of early hominid phylogeny. *J. hum. Evol.* **32,** 17–82.
Swisher III, C. C., Curtis, G. H., Jacob, T., Getty, A. G., Suprijo, A. & Widiasmoro (1994). Age of the earliest hominids in Java, Indonesia. *Science* **263,** 1118–1121.
Tobias, P. V. (1967). *Olduvai Gorge, Volume 2 The Cranium and Maxillary Dentition of Australopithecus (Zinjanthropus) boisei*. Cambridge: Cambridge University Press.
Tobias, P. V. (1997). Evolution of brain size, morphological restructuring and longevity in early hominids. In (S. U. Dani, A. Hori & G. F. Walter, Eds) *Principles of Neural Aging*, pp. 153–174. Amsterdam: Elsevier.
Walker, A. C., Leakey, R. E., Harris, J. M. & Brown, F. H. (1986). 2·5-Myr *Australopithecus boisei* from west of Lake Turkana, Kenya. *Nature* **322,** 517–522.
Weber, G. W., Recheis, W., Scholze, T. & Seidler, H. (1998). Virtual anthropology (VA): methodological aspects of linear and volume measurements—first results. *Coll. Antropol.* **22,** 575–583.

Appendix

Endocasts were reconstructed for four *Paranthropus* specimens and their cranial capacities determined by JG in consultation with DF. The procedures for reconstructing each specimen and determining its cranial capacity are described below.

SK 1585

The natural SK 1585 endocast of *P. robustus* from Swartkrans, South Africa, reproduces most of the right hemisphere, except for a small portion at the rostral end of the frontal lobe (Figure 4). DF studied the original specimen, made a replica of it, and verified that the replica corresponded metrically to the original. Available aspects of the SK 1585 endocast reveal features of both the occipital sinus and the superior sagittal sinus extending without interruption to within 6 mm of bregma. The right temporal pole is

intact and resembles the temporal poles of KNM-WT 17000 and KNM-WT 17400, differing dramatically from the temporal poles of Sts 5, Sts 19, Sts 60, and Stw 505. Extension of the midline provides a reliable site along which to reconstruct the pole of the frontal lobe which is otherwise largely intact including the orbital surface. We reconstructed the missing portion of the frontal lobe directly on this replica, using unreconstructed portions of endocasts from *Paranthropus* specimens OH 5, KNM-WT 17400, and KNM-WT 17000 as models for the shape. The latter two specimens (Leakey & Walker, 1988) were not available in 1972 when SK 1585 was first reconstructed (Holloway, 1972). Although OH 5 (which was available) reproduces the dorsal surface of rostral frontal lobe, it lacks the orbital surface. We molded our reconstruction to fit the natural contours of the available portions of SK 1585's frontal lobe. As described for the 1972 reconstruction (Holloway, 1972), we reconstructed the hypophysial region and the inferior surface of the medulla to the border of the foramen magnum (referring especially to OH 5 and KNM-WT 17000), and filled in a few minor pits and depressions (Figure 4).

After the general shape of the right hemisphere of the SK 1585 endocast was reconstructed, we made a silicone mold of it to the midline. Although the cleft between the inferior border of the temporal lobe and the cerebellum (i.e., the space normally occupied by the petrous pyramid) is filled medially with matrix, the lateral portion of this cleft reproduces the brain nicely (Figure 4). We measured the surface dimensions of the extraneous matrix, the depth of its lateral extent, and the length of the intact portion of the cleft with calipers. These measurements, together with observation of the intact (left) side of the comparable region in OH 5, were used to reconstruct the shape of the cleft in plasticine, which was then fitted into the appropriate place within the mold of our reconstruction, effectively reproducing the missing portion of the petrous pyramid while subtracting the extraneous matrix. This mold was used to produce a final silicone copy. To obtain a cranial capacity, we filled this mold with water and measured its volume in a graduated cylinder and doubled the measurement to represent both sides of the reconstructed endocast.

OH 5

We first compared our copy of an endocast (copied by DF at the National Museums of Kenya) from the original reconstructed skull of OH 5 to silicone impressions prepared from the interior surfaces of Wenner-Gren casts of five cranial fragments that, when reassembled, reproduce much of the braincase of the skull. The fragments include the rostral end of the dorsal surface of the frontal bone on both sides, a large fragment that reproduces both parietals, two fragments representing the petrous temporals, and the occipital bone. After we verified that the impressions from the individual fragments metrically and visually reproduced the details revealed on the endocast from Nairobi, we coated the internal surfaces (i.e., the braincase) of each of the five cranial fragments with a silicone rubber to which we added russet pigment. We then reconstructed the cranium from the coated cranial fragments using plasticine to compensate for missing portions that would be reconstructed in subsequent steps. In modeling our reconstruction of the skull, we followed the natural contours of the available cranial fragments. We then cast the entire braincase using unpigmented silicone. After the silicone cured, we disarticulated the cranium. The resulting endocast was pigmented russet in areas that reproduced the internal surfaces of cranial fragments and white in other reconstructed regions. We proceeded to refine the white areas of the endocast, while remaining faithful to the overall size and contours, by referring to the

unreconstructed portions of *Paranthropus* endocasts SK 1585, KNM-WT 17000, KNM-WT 17400, KNM-ER 732, and KNM-ER 23000. (We also compared the general shape of our reconstructed endocast with that seen in photographs of the endocast of KNM-ER 13750, Leakey & Walker, 1988).

The orbital surface in the region of the nasal rostrum required sculpting with silicone sealant in order to reflect the typical beaked-shape and relative size of KNM-WT 17400 and KNM-WT 17000. Dorsal views of these two endocasts, KNM-ER 23000, and a photograph of KNM-ER 13750 were used to reconstruct the area between the rostral region of the frontal lobe and the posterior two-thirds of the braincase [Figure 3(b)]. The anterior portions of the temporal lobes (Figure 4) were reconstructed based on the morphology of SK 1585, KNM-WT 17000, and KNM-WT 17400. After we were satisfied that our reconstructed endocast was as true to the known morphology of other *Paranthropus* endocasts as possible, we compared it with measurements and drawings provided for an earlier reconstruction of the endocast (Tobias, 1967). Our overall measurements and those provided earlier (Tobias, 1967:92) varied by less than 1%. Finally, a master mold was cast in plaster and used to pour a final silicone endocast. A cranial capacity was determined by filling our reconstructed endocast with latex foam and water displacing it. Due to the completeness of the original calvarium, we have the highest confidence in our endocast reconstruction and cranial capacity.

KNM-ER 732

We coated the portions of the interior of a cast of this specimen (acquired from the National Museums of Kenya) that reproduce morphology of the cerebral cortex with pigmented silicone. A clearly visible frontal crest arcs posteriorly into the sulcus that lodges the superior sagittal sinus, which together comprise an arc of approximately 5·7 cm. The midline of the endocast was determined by projecting straight back from the caudal end of the visible portion of the sulcus. The partial right hemicranium was then cast to the midline with white silicone, and the resulting hemi-endocast was color-coded as described for OH 5. This specimen was then compared metrically and visually to a copy of an endocast that was prepared from the original fossil (acquired by D.F. in Nairobi). Once we were assured that the silicone endocast maintained the integrity of the original specimen, we proceeded to reconstruct the missing portions. These included most of the orbital surface and part of the lateral surface of the frontal lobe, anterior end of the temporal lobe, large portions of the parietal lobe, and virtually all of the occipital lobe and cerebellum (Figure 4). Reconstructions of the frontal and temporal lobes were based on the same comparative specimens used to reconstruct these regions in OH 5. The remaining portions were reconstructed by referring to the unreconstructed portions of SK 1585, KNM-WT 17000, KNM-WT 17400, and KNM-ER 23000. The completed reconstruction was filled with latex foam for rigidity and then cast in plaster, and that mold was used to yield a final silicone copy. The cranial capacity estimate was obtained by filling the plaster mold with water which was measured in a graduated cylinder, and doubled.

KNM-ER 407

The approach to this reconstruction involved the alignment of four cranial fragments that, in addition to providing a significant length of the sulcus for the superior sagittal sinus, also provide bilateral features of the coronal suture that could be projected to intersect the midline at bregma. It is also fortunate that aspects of the lambdoidal

suture are apparent for both hemispheres in addition to the groove for the left occipital sinus as these features inform a reconstruction with confidence. We coated the internal surfaces of casts of fragments of the cranium obtained from the National Museums of Kenya with pigmented silicone, articulated the fragments using plasticine to compensate for the missing portions, and then cast the entire braincase with white silicone. The midline for the anterior portion of this specimen was determined in the same manner as it was for SK 1585, using the same available landmarks. We confirmed that the pigmented portions of the resulting endocast maintained the integrity of the original specimen by comparing it with the comparable aspects on an endocast that was reconstructed using the original fossil (Falk & Kasinga, 1983). We then proceeded to reconstruct the missing portions on the left side which included the anterior end of the temporal, and the rostral end of the frontal lobe, compensating for fractures and distortions reproduced from the reconstructed cranium. For reference, we used appropriate unreconstructed portions of endocasts from KNM-WT 17000, KNM-WT 17400, OH 5, and SK 1585 (right hemisphere). The completed hemicast (Figure 4) was then cast in plaster, and that mold was used to yield a final silicone copy. A cranial capacity was obtained by filling the mold with water and doubling its measured volume.